Proceedings of Ninth World Conference on Earthquake Engineering
August 2-9, 1988, Tokyo-Kyoto, JAPAN (Vol.IV)

6-5-20

# DIAPHRAGM BEHAVIOR OF REINFORCED CONCRETE FLOOR SLABS

Sheng-Jin CHEN[1], Ti HUANG[2], and Le-Wu LU[2]

[1]Department of Construction Engineering,
National Taiwan Institute of Technology,
Taipei, Taiwan, R.O.C.
[2]Department of Civil Engineering, Lehigh University,
Bethlehem, Pennsylvania, U.S.A.

## SUMMARY

The diaphragm characteristics of three commonly used reinforced concrete floor systems have been studied both experimentally and analytically. They are: flat plates supported on columns, slabs supported on beams, and waffle slabs. Many important parameters, such as the stiffness, strength and deformation capacity, in both the elastic and post-elastic range, have been incorporated into the test program. These characteristics are fundamental in the study of diaphragm behavior of floor systems and its effect on building structural response.

## INTRODUCTION

In current design practice of building structures, the floor slabs are usually designed for vertical gravity loads only. However, for building structure subjected to earthquake loading, the floor slabs also serve the important function of connecting all vertical elements together and distributing the inertia forces to the lateral load resisting systems, such as shear walls and frames. This behavior is usually referred as the diaphragm action and is basically governed by the in-plane characteristics of the floor systems. For structures in which the stiffness of the floor and the vertical system do not differ greatly diaphragm deformation of the floors must be explicitly considered in the analysis, and the information on in-plane deformation of the floor system becomes very crucial.

## EXPERIMENTAL AND ANALYTICAL PROGRAM

A series of tests were conducted for the purpose of examining the in-plane behavior of floor slabs. Two specimens were constructed for each of the three slab types: flat plate (Refs. 1, 2), beam-supported slab (Refs. 3, 4) and waffle slab (Refs. 5, 6). Each of the test specimens contained three consecutive square panels supported on two interior shear walls and four columns. All specimens had the same planar dimensions. The slab thickness varied among the several systems, but all were designed for the same live gravity load. Fig. 1 show the detailed dimensions of the waffle slab specimen. Each panel formed the basic testing unit and was tested as an individual structure. The test panel was supported on one side by a fixed shear wall and free to undergo in-plane movement along the other edges. The in-plane shear load was applied along the column line parallel but

opposite to the shear wall, while the uniform vertical load when used, was simulated by equivalent point loads (Fig. 2).

Two different shear spans were selected for each slab system: 1,630 mm for side panels and 3,260 mm for the middle panel. The key information obtained from these tests was the load-displacement relationship of the test panel, including the initial elastic stiffness, ultimate load capacity, and ultimate displacement capacity. The panels were tested with four types of loading sequence: (1) Monotonic in-plane load, (2) Monotonic in-plane load and service gravity load, (3) Cyclic in-plane load controlled by preselected displacement amplitudes and (4) Cyclic in-plane load and service gravity load. In (2) and (4), the full service gravity load was applied first and the in-plane shear load followed. Thus, the test panels were subjected to combined action of the full gravity load and varying in-plane shear load. The objective of (3) and (4) was to study the degradation of stiffness and strength under repeated and reversed in-plane loading. The results of these tests are given in Tables 1 and 2.

The finite element model used in the analytical study consists of two-dimensional plane stress elements representing concrete, and truss elements representing reinforcing bars (Ref. 7). An elastic-perfect-plastic material model is selected for the steel. For concrete under plane stress, the Mohr-Coulomb criterion with tension cut-off is used. If failure occurs in the compression region, the concrete is assumed to be crushed and its stiffness is lost completely. The stiffness thus lost is not regained by unloading. The rate of stress release after crushing follows the descending slope of the post-peak portion. However, to prevent numerical difficulty the stiffness of the material on the descending portion of the stress-strain curve is taken to be zero. For concrete under tension, the smeared cracking model is used for simulation of cracked concrete. After cracking has occurred, the normal stress across the crack is released completely, but part of the shear resistance is retained on account of aggregate interlocking. The material becomes anisotropic after cracking. The stiffness normal to the crack is assumed to be totally lost, while the shear stiffness along the crack is reduced. This effect can be represented by means of a shear stiffness retaining factor. The stiffness in the direction parallel to the crack is also reduced and is represented by a stiffness softening factor. Results of finite element analyses using this model are given in Table 5.

## COMPARISON OF RESULTS

Table 1 lists the initial stiffness from experimental results, finite element analysis and beam analogy of a single panel. Experimentally, the presence of service vertical load caused a significant decrease in the initial stiffness. This was explained by the fact that these specimens were cracked by vertical load before the application of the in-plane load. Neither the SAP IV solution nor the beam analogy includes the effect of cracking due to out-of-plane loading.

Under in-plane load the slab panel behaved like a deep cantilever beam. The in-plane ultimate strength was influenced by the nature of loading (monotonic or cyclic), the moment-to-shear (span-to-depth) ratio, and the intensity of vertical load. In all cases the ultimate strength was reached after the development of a major crack which extended parallel to the shear wall at the location where a number of negative reinforcing bars were terminated. After the formation of this major crack, the overall deformation of the panel was controlled primarily by the opening and closing of the major crack, with few new crack developing. The section at the major crack acted like a plastic hinge. The opening of the major crack also caused a reduction of the size of the compression region. Several

panels finally failed by rupture of reinforcing bars in the tension side and crushing of concrete in the compression region.

In Table 3 are listed the yield displacements $\delta_y$, ultimate displacements $\delta_u$, and the ductility factors, D, of various test specimens. The total displacements $\delta_t$, which are the sum of the ultimate displacements in the two directions are also given. The total displacement can be viewed as an indication of the deformability of the test slab.

The slabs tested under cyclic loading showed lower ultimate strength as compared with those tested under monotonic load. This is due to the damage accumulated during repeated load reversals. Table 4 shows the ratio of the ultimate load under cyclic loading to that under monotonic loading. The strength reduction due to cyclic loading was 17 to 26% for beam-supported slabs, and 14% for flat plates. As for waffle slabs, the reduction of strength was less than 5% and may be ignored. Also listed in Table 4 are comparisons of deformability, which is related to the total displacement. The total displacements of the cyclic loading cases are smaller than those of monotonic cases, with a reduction as high as 40%.

The basic behavior of slabs tested with gravity load was very similar to that without gravity load. The crack pattern and ultimate deflection capacity were about the same. The effect of shear span on the ultimate in-plane strength was studied by doubling the moment-to-shear ratio and calculating the ratio of ultimate load for the paired specimens. For BH3MN/BH2MN, this ratio was found to be 0.47 and 0.44, respectively, for positive and negative loading. Corresponding values were 0.42 and 0.44 for BH3CY/BH1CY, 0.45 and 0.44 for FH2CY/FH3CY, and 0.56 and 0.46 for WH3MN/WH1MN. Almost all these ratios were somewhat lower than the 0.50 ratio of the moment arm. It was felt that the location of the major crack had an important influence on the ultimate strength. The ratios of distances from the loading line to the major crack were 0.43 for both slabs on beams and flat plates, and 0.40 for waffle slabs. In general, the in-plane strength of the tested floor panels was governed by the major cracks, with the bending strengths at the major crack and at the fixed support providing upper and lower bound values, respectively. The doubling of the moment-to-shear ratio was found to increase the ductility considerably (Table 5). This increase in ductility may be viewed as a consequence of the different crack patterns in these specimens. An examination of the crack pattern showed that for a depth-to-span ratio of 0.75 the cracks were mostly of the diagonal type, while for a higher ratio of 1.5, the cracks were dominated by the shear-flexure type. As the opening of the flexural cracks and the yielding of reinforcing bars contributed significantly to the plastic deformation of the slab panel, the observed increase of ductility with the moment-to-shear ratio was understandable.

## CONCLUSIONS

1. The presence of full service gravity load caused a decrease of about 10% in the in-plane strength for cyclic load, and 20% for monotonic load. However, the displacement capacity was not seriously affected. The general behavior of the slabs was not altered by the vertical load, and the major crack still developed along the boundary between the column and middle strips, with the complete formation of the major crack governing the ultimate resistance.
2. Cyclic loading led to more distributed cracks and plastic deformation but did not change the development of the major crack.
3. Cyclic loading caused reduction of the in-plane strength and the displacement capacity of a floor panel. The reduction in strength was less than 30% for slab-on-beams and flat plate. For waffle slab, this reduction was less than 5%.

4. In-plane strength of the slab panels was basically controlled by the flexure strength at the major crack. In all cases, the major crack was started from where many of the negative reinforcing bars in the column strips were terminated.

5. Waffle slab exhibited larger ductility as compared with flat plate and slab-on-beams.

6. The finite element model developed in this study, although relatively simple, is able to simulate adequately the stiffness, strength, and deformability of floor slabs under in-plane load.

## ACKNOWLEDGMENTS

This research was part of a general investigation on diaphragm behaviors of floor systems supported by a grant from National Science Foundation (No. CEE8120589) to Lehigh University. Drs. H. F. Karadogan, M. Nakashima and Mr. X. Ji were in charge of the experimental programs at various stages.

## REFERENCES

1. Karadogan, H. F., Huang, T., Lu, L. W., and Nakashima, M., "Behavior of Flat Plate Floor Systems under In-Plane Seismic Loading,"Proceedings of the 7th WCEE, Istanbul, Turkey, September 1980, pp. 9-16.
2. Karadogan, H. F., Lu, L. W., and Huang, T., "Techniques for In-Plane Vibration and Shear Testing of Model Floor Slabs," Symposium on Dynamic Modeling of Concrete Structures, Detroit, ACI SP-73, 1982, pp. 189-204.
3. Nakashima, M., "Seismic Resistance Characteristics of Reinforced Concrete Beam-Supported Floor Slabs in Building Structures," Ph.D. thesis, Lehigh University, March 1981.
4. Nakashima, M., Huang, T., and Lu, L. W., "Experimental Study of Beam-Supported Slabs under In-Plane Loading," Journal of the American Concrete Institute, Vol. 79, No. 1, January - February 1982, pp. 59-65.
5. Ji, X., Huang, T., Lu, L. W., and Chen, S. J., "An Experimental Study of the In-Plane Characteristics of Waffle Slab Panels," Fritz Engineering Laboratory Report No. 481.3, Lehigh University, To be published.
6. Ji, X., Chen, S. J., Huang, T., and Lu, L. W., "Deflection of Waffle Slabs under Gravity and In-Plane Loads," Deflection of Concrete Structures, ACI SP-86, Detroit, 1985, pp. 283-294.
7. Chen, S. J., Huang, T., and Lu, L. W., "Nonlinear Analysis of RC Panels under In-Plane Loading," American Society of Civil Engineers, Ninth Conference on Electronic Computation, Birmingham, Alabama, February, 1986.

Table 1 Initial In-Plane Stiffness of Individual Panels

| | Experimental | SAP4 | Beam Analogy |
|---|---|---|---|
| BH2MN | 218 | 326 | 320 |
| BH1CY | 272 | 326 | 320 |
| BH3MN | 166 | 206 | 202 |
| BH3CY | 175 | 216 | 212 |
| BV1MN | 222 | 340 | 334 |
| BV2CY | 201 | 340 | 334 |
| WH1MN | 165 | 199 | 186 |
| WV2MN | 119 | 187 | 172 |
| WH2CY | 167 | 199 | 186 |
| WV1CY | 73 | 187 | 172 |
| WH3MN | 33 | 102 | 117 |
| FH5MN | 65 | 240 | 244 |

Unit: MN/m

Table 2 Strength Test Results

| | $+P_u$(kN) | $-P_u$(kN) | $+\delta_u$(mm) | $-\delta_u$(mm) |
|---|---|---|---|---|
| FH5MN | 76.5 | - 54.6 | 11.2 | 4.79 |
| BH2MN | 120.0 | - 88.5 | 7.62 | 7.24 |
| BH3MN | 56.9 | - 38.7 | 7.11 | 5.72 |
| WH1MN | 98.4 | - 98.1 | 6.81 | 11.73 |
| WH3MN | 55.5 | - 45.5 | 21.2 | 23.8 |
| FV1MN | 131.3 | -101.5 | 4.98 | 1.93 |
| BV1MN | 102.0 | - 89.8 | 9.22 | 9.22 |
| WV2MN | 95.1 | - 84.6 | 10.5 | 13.6 |
| FH3CY | 70.8 | - 63.2 | 3.51 | 2.87 |
| BH1CY | 94.7 | - 96.5 | 6.75 | 6.30 |
| BH3CY | 41.8 | - 40.5 | 4.60 | 5.42 |
| WH2CY | 93.7 | - 88.5 | 8.32 | 9.55 |
| BV2CY | 85.0 | - 83.2 | 6.27 | 5.08 |
| FV2CY | 147.7 | -128.6 | 3.33 | 1.91 |
| WV1CY | 94.4 | - 81.4 | 7.28 | 7.25 |

Table 3 Ductility Factors

| | $\delta_y$(mm) | $\delta_u$(mm) | $-\delta_u$(mm) | $\delta_t$(mm) | D | -D |
|---|---|---|---|---|---|---|
| FH5MN | 3.16 | 11.2 | 4.79 | 16.0 | 3.5 | 1.5 |
| BH2MN | 2.06 | 7.62 | 7.24 | 14.86 | 3.7 | 3.5 |
| BH3MN | 1.44 | 7.11 | 5.72 | 12.83 | 4.9 | 4.0 |
| WH1MN | 2.08 | 6.81 | 11.73 | 18.54 | 3.3 | 5.6 |
| WH3MN | 3.40 | 21.2 | 23.8 | 45.0 | 6.2 | 7.0 |
| FV1MN | 1.04 | 4.98 | 1.93 | 6.9 | 4.8 | 1.9 |
| BV1MN | 2.92 | 9.22 | 9.22 | 18.44 | 3.2 | 3.2 |
| WV2MN | 2.47 | 10.5 | 13.6 | 24.1 | 4.3 | 5.5 |
| FH3CY | 1.61 | 3.51 | 2.87 | 6.38 | 2.2 | 1.8 |
| BH1CY | 2.81 | 6.75 | 6.30 | 13.05 | 2.4 | 2.2 |
| BH3CY | 2.47 | 4.6 | 5.42 | 10.02 | 1.9 | 2.2 |
| WH2CY | 1.40 | 8.32 | 9.55 | 17.87 | 5.9 | 6.8 |
| BV2CY | 2.19 | 6.27 | 5.08 | 11.35 | 2.9 | 2.3 |
| FV2CY | 1.33 | 3.33 | 1.91 | 5.24 | 2.5 | 1.4 |
| WV1CY | 2.31 | 7.28 | 7.25 | 14.53 | 3.2 | 3.1 |

Table 4 Comparison of Monotonic Load and Cyclic Load

| | Strength | Deformability |
|---|---|---|
| FH3CY/FH3MN | 0.855 | |
| BH1CY/BH2MN | 0.789 | 0.878 |
| BH3CY/BH3MN | 0.735 | 0.781 |
| BV2CY/BV1MN | 0.833 | 0.616 |
| WH2CY/WH1MN | 0.952 | 0.964 |
| WV1CY/WV2MN | 0.993 | 0.603 |

Table 5 Ultimate Load and Deflection

| | $P_{u,exp}$ (kN) | $P_{u,ana}$ (kN) | $P_{u,beam}$ (kN) | $\delta_{u,exp}$ (mm) | $\delta_{u,ana}$ (mm) | $\delta_{u,beam}$ (mm) |
|---|---|---|---|---|---|---|
| H1MN | 160 | 169 | 154 | -- | 2.85 | 7.7 |
| FH3MN | 82.8 | 77.9 | 66.3 | -- | 1.12 | 10.3 |
| FH5MN | 76.5 | 84.6 | 74.3 | 11.2 | 6.51 | 10.6 |
| BH2MN | 120 | 118 | 108 | 7.62 | 8.09 | 5.5 |
| BH3MN | 56.9 | 55.6 | 50.3 | 7.11 | 6.42 | 8.4 |
| WH1MN | 98.4 | 102.4 | 120.6 | 6.81 | 7.28 | 6.9 |
| WH3MN | 55.5 | 47.8 | 53.8 | 21.2 | 4.48 | 10.4 |

Note: The subscripts exp, ana and beam denote, respectively, the experimental, analytical (by FEM) and beam model values.

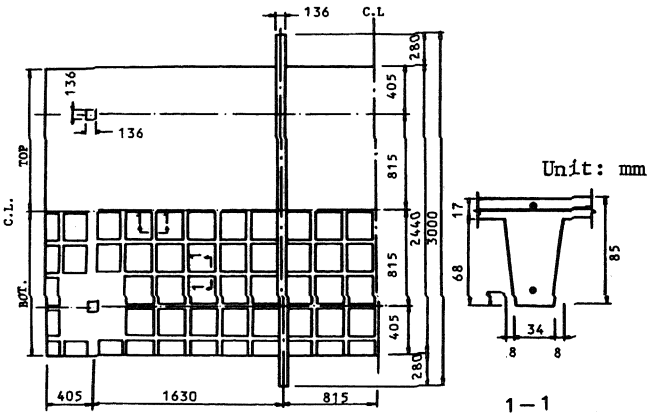


Fig. 1. Detailed dimension of waffle slab.

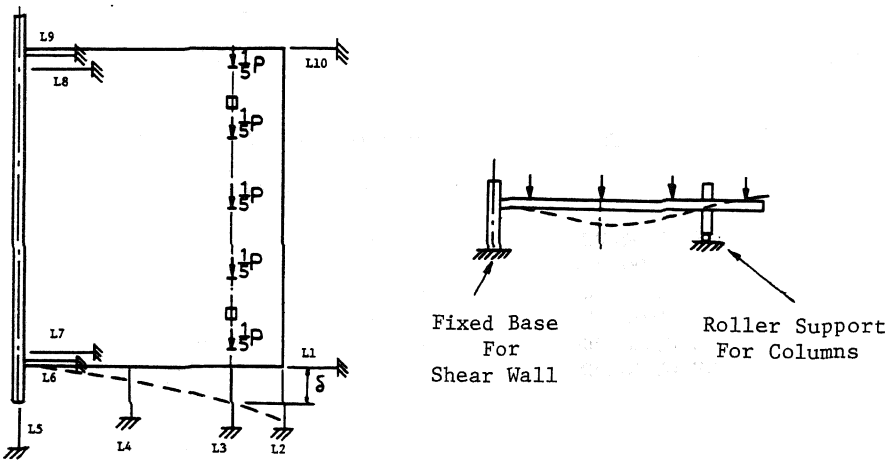


Fig. 2. Load and LVDT arrangement in strength test.